BAREKENG: Journal of Mathematics and Its Applications
September 2024 Volume 18 Issue 3 Page 1509–1518
P-ISSN: 1978-7227 E-ISSN: 2615-3017
https://doi.org/10.30598/barekengvol18iss3pp1509-1518

NUMERICAL COMPUTATION OF ONE- AND TWO-LAYER SHALLOW FLOW MODEL

K. Dharmawan[1*], P. V. Swastika[2], G.K Gandhiadi[3]

[1,2,3]*Department of Mathematics, Faculty of Mathematics and Natural Sciences, Universitas Udayana*
Jl. Raya Kampus UNUD, Bukit Jimbaran, Bali 803611, Indonesia

*Corresponding author's e-mail: * **k.dharmawan@unud.ac.id***

Article History:

Received: 26th November 2023
Revised: 5th January 2024
Accepted: 16th June 2024
Published: 1st September 2024

Keywords:

Saint Venant;
Dam-Break;
Sub-Maximal Exchange;
Momentum-Conserving
Staggered-Grid.

ABSTRACT

In this research, we study a proficient computational model designed to simulate shallow flows involving one- and two-layer shallow flow. This numerical model is built upon the Saint Venant equations, which are widely used in hydraulics to depict the behavior of shallow water flow. The numerical scheme used here is constructed based on the conventional leapfrog technique implemented on a staggered grid framework, referred to as MCS. The primary objective of this research is to re-examine and implement the MCS in accurately modelling the free surface and interface waves produced by different flows passing through irregular geometries. Unlike the conventional MCS, we modify the momentum conservation principle to be more general, accommodating a non-negative wet cross-sectional area due to irregular geometry. We successfully conduct numerous numerical simulations by examining various scenarios involving one-layer and two-layer flow through irregularly shaped channels or structures. Our results show that the correct surface wave profile generated by a one-dimensional dam break through the triangular obstacle in the open channel can be simulated very well. Comparison with the existing experimental data seems promising although some disparities are being found due to dispersive phenomena with RMSE less than 5%. Furthermore, our scheme is successfully extended to simulate the steady sub-maximal exchange in two-layer flows using specific boundary conditions. The alignment between the submaximal numerical results with exchange flow theory is noticeable in the interface profile, characteristics of flow conditions and the flux values achieved when the steady situation occurs. These satisfying results indicate that our proposed numerical model can be used for practical needs involving various flow situations both one and two-layer cases

How to cite this article:

K. Dharmawan, P.V Swastika and G.K. Gandhiadi, "NUMERICAL COMPUTATION OF ONE- AND TWO-LAYER SHALLOW FLOW MODEL," *BAREKENG: J. Math. & App.*, vol. 18, iss. 3, pp. 1509-1518, September, 2024.

Journal homepage: *https://ojs3.unpatti.ac.id/index.php/barekeng/*
Journal e-mail: *barekeng.math@yahoo.com; barekeng.journal@mail.unpatti.ac.id*
Research Article · Open Access

1. INTRODUCTION

The Non-Linear Shallow Water Equation (NLSWE) stands as a versatile mathematical model with extensive applications across different fields. Its ability to capture the complex behaviors of fluid in shallow environments makes it invaluable in various engineering applications, from coastal and hydraulic engineering to understanding and mitigating risks associated with water-related disasters. One of the primary strengths of the NLSWE lies in its ability to represent and predict the dynamics of different phenomena. For instance, it proves useful in understanding internal wave generation within narrow straits [1][2][3]. These internal waves, often occurring in regions with varying depths, have significant implications for oceanographic processes and the distribution of water properties. Additionally, the NLSWE finds application in studying coastal phenomena [4] which encompass a range of dynamic processes along coastlines, including wave propagation, tides, and storm surges. Its utility extends to hydraulic flow scenarios [5][6][7], where the equation aids in modelling water flow within pipes, channels, or hydraulic systems, critical in various engineering designs. Furthermore, the equation's capability extends to understanding and predicting the behavior of water level generated from catastrophic events like hydro dam failures [8][9][10][11].

Extensive investigation has been carried out in order to obtained a solution to NLWSE. So far, only few accurate solutions to the NLSWE have been discovered, the majority of which describe basic flows in idealized situations [12]. This constitutes a significant barrier in terms of applications that no one has yet been able to overcome. As a result, it is necessary to developing robust and reliable model to solve NLSWE in real-world situations.

Several authors have been conducted comprehensive research on numerical models for solving NLSWE, one of which is using the finite difference method. Recently there has been very rapid development in the use of finite difference such us; A Q-scheme of Roe upwinding [13], Lax-Fredrich [14], Lax-Wendroff [15], staggered conservative scheme [16], etc. Stelling and Duinmeijer [16], extend Arakawa C-grid [15], and allows the use of conservation of energy or momentum locally. In our previous work we focus only on the development of momentum conservative principle to approximate the advection term [4][17][18][19][20][21], which is the reason for the name of momentum conserving staggered-grid (MCS) scheme.

The MCS employs by utilizing the conventional leapfrog technique implemented on a staggered grid framework. It discretizes the nonlinear aspects through a conservative approach. This means it employs methods that prioritize conservation, such as employing momentum-conserving approximations for handling advection terms within the momentum equation. Additionally, it utilizes upwind approximations for managing the nonlinear term in the mass continuity equation [19]. The method has been demonstrated to be explicit, effective, devoid of numerical damping, and doesn't necessitate a Riemann solver for flux calculation. Therefore, it is computationally efficient.

Thus, the aim in this manuscript is to re-examine and implement the momentum-conserving staggered-grid (MCS) scheme to address different problems within both single-layer and two-layer fluid systems. The process begins by outlining the governing equations for these systems in Section 2. This section lays the groundwork by defining the equations that govern the behavior of both the single-layer and two-layer fluid systems. Section 3 delves into a detailed revisit of the MCS scheme itself. In Section 4, the study proceeds to conduct benchmark tests. These tests involve comparing the computed results obtained using the MCS scheme with experimental data. The objective here is to evaluate and analyze how accurately the MCS scheme models and predicts the behavior of the fluid systems. This comparison helps in assessing the reliability and robustness of the scheme in practical scenarios. Finally, in Section 5, the discussion reaches its conclusion. This section summarizes the findings, draws conclusions from the benchmark tests, and includes overall remarks about the performance and effectiveness of the MCS scheme in addressing the complexities of the single-layer and two-layer fluid systems. It serves as the concluding part that encapsulates the key takeaways and insights obtained throughout the study.

2. RESEARCH METHODS

The research method used in this article combines literature reviews, case studies, quantitative methods, simulation and modelling. Initially, literature, including books, articles, and journals, is reviewed

to govern the behavior of fluid flows in shallow environments, such as irregularly shaped channels. This mathematical model is based on the Saint Venant equations (a variant of NLSWE), commonly used in hydraulics for shallow water flow in open channels. Next, a literature study was also carried out to choose an appropriate numerical method that was used to solve the case study to be discussed. A numerical model is then constructed using MATLAB software and the MCS algorithm to model the one- and two-layer fluid system and predict its behavior under various conditions. Quantitative methods are used to analyze the numerical results, aiming to match the comparative data. The comparative data for the one-layer fluid case is taken from a dam-break experiment **[22]**, while the two-layer fluid case is based on sub maximal exchange theory on **[23]**.

2.1 One Layer Shallow Flow

In this part, we present the one-layer shallow model, which is used to simulate the free surface waves as sketched in **Figure 1 (a)**. Suppose a fluid layer bounded below by a topography $d(x)$ and above by the free surface $\eta(x,t)$, flowing through an open channel with a rectangular cross-section. The motion of the free surface is governed by the one-layer Saint Venant equations given by the followings

$$\frac{\partial A}{\partial t}+\frac{\partial Q}{\partial x}=0 \tag{1}$$

$$\frac{\partial u}{\partial t}+u\frac{\partial u}{\partial x}+g\frac{\partial (h+d)}{\partial x}=0 \tag{2}$$

The notations $h(x,t)$ represents the fluid height, $Q(x,t)$ is flux. Note that $Q(x,t)=A(x,t)u(x,t)$, with $u(x,t)$ is the horizontal fluid velocity. **Equation (1)** and **Equation (2)** will be used for simulation of one-layer cases.

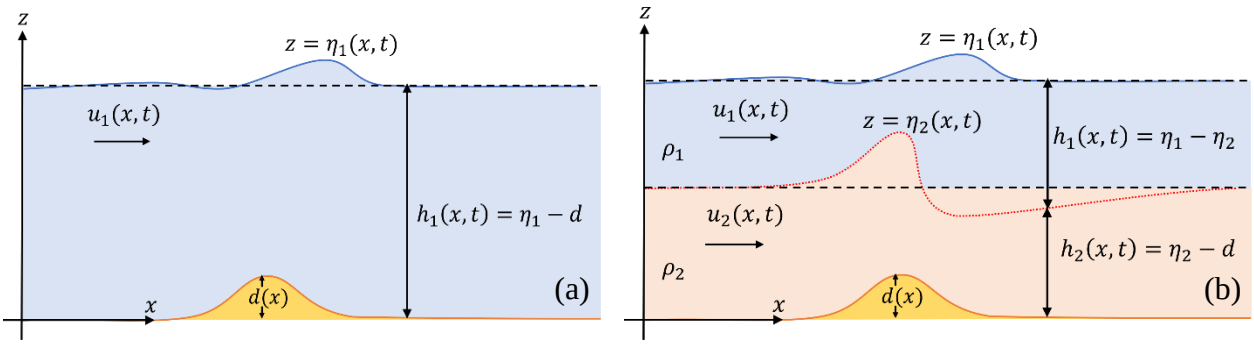

Figure 1. Sketch of Computational Domain and Notation; (a) for One-Layer; (b) for Two Layer.

2.2 Two Layer Shallow Flow

Suppose a fluid layer bounded below by a topography $d(x)$ and above by the free surface $\eta(x,t)$, flowing through an open channel with a rectangular cross-section. The fluids as sketched in **Figure 1 (b)**, consist of two immiscible waters with different densities. The two-layer Saint Venant equations govern the motion of the free surface and interface given by the following set of equations.

$$\frac{\partial A_1}{\partial t}+\frac{\partial Q_1}{\partial x}=0 \tag{3}$$

$$\frac{\partial u_1}{\partial t}+u_1\frac{\partial u_1}{\partial x}+\frac{1}{\sigma}\frac{\partial}{\partial x}(h_1+h_2)=0 \tag{4}$$

$$\frac{\partial A_2}{\partial t}+\frac{\partial Q_2}{\partial x}=0 \tag{5}$$

$$\frac{\partial u_2}{\partial t}+u_2\frac{\partial u_2}{\partial x}-\frac{\partial h_1}{\partial x}+\frac{1}{\sigma}\frac{\partial}{\partial x}(h_1+h_2+d)=0 \tag{6}$$

where $\sigma = 1 - r$ and $r = \rho_1/\rho_2$ is the ratio of the densities. In the above equations, variables $Q_i = A_i u_i$ represent the discharge for each layer whereas A_i denote the wet cross-sectional area of each layer. The **Equation (3)** - **Equation (6)** is the depth average of Euler equations written in the form of balance laws, applicable for nearly horizontal flows, which are hydrostatic, and frictionless. Further, we will use the following relation $\eta_1 = h_1 + h_2$ and $\eta_2 = h_2 + d$. The **Equation (3)** - **Equation (6)** will be used for simulation of two-layer cases.

2.3 Numerical Scheme

In this subsection, we revisit MCS scheme as discussed in **[17]**, **[18]** to solve both one layer and two-layer model. The MCS scheme is basically a leapfrog method applied in staggered grid framework where the momentum-conservative principle, proposed by Stelling and Duinmeijer **[16]**, are used to discretized the advective (non-linear) term.

Suppose the spatial domain $-L \le x \le L$ is uniformly discretized by half-step partition intervals, resulting in a staggered grid domain with partition points:

$$-L = x_{\frac{1}{2}}, x_1, \cdots, x_{j-\frac{1}{2}}, x_j, x_{j+\frac{1}{2}}, \cdots, x_{N+\frac{1}{2}} = L$$

with $N = \frac{2L}{\Delta x}$. This staggered arrangement allows us to alternately calculate the unknown variables on adjacent grid points. Thus, the numerical approximation for one-layer cases in **Equation (1)** and **Equation (2)** read as,

$$\frac{dA_j^n}{dt} + \frac{Q^n_{j+\frac{1}{2}} - Q^n_{j-\frac{1}{2}}}{\Delta x} = 0 \tag{7}$$

$$\frac{du^n_{j+\frac{1}{2}}}{dt} + (u\partial_x u)^n_{j+\frac{1}{2}} + g\left(\frac{\eta^{n+1}_{j+1} - \eta^{n+1}_j}{\Delta x}\right) = 0 \tag{8}$$

where $\eta_j = h_j + d_j$. The numerical flux $Q^n_{j+1/2}$ can be approximated by upwind method that will be described later as well as the advective term $(u\partial_x u)$. The fully discrete scheme of **Equation (7)** and **Equation (8)** can be obtained by using a standard ODE solver w.r.t of time t variable.

Furthermore, there are many numerical techniques to approximate the advective term $(u\partial_x u)$, meanwhile, here we adopt the momentum conservative principle first proposed in **[16]**

$$(u\partial_x u) = \frac{1}{h}(Qu)_x - (uQ_x) \tag{9}$$

Since the channel wall is irregular involving non-negative wet-cross sectional area A, rather than using the conventional momentum conservative principle as in **[24]**, **[25]**, here we modify the **Equation (9)** to get the discrete approach of modified momentum conservative principle as given by the following

$$(u\partial_x u)^n_{j+\frac{1}{2}} = \frac{1}{\bar{A}^n_{j+\frac{1}{2}}}\left(\frac{\bar{Q}^n_{j+1}\,\overset{*}{\square}u^n_{j+1} - \bar{Q}^n_j\,\overset{*}{\square}u^n_j}{\Delta x} - u^n_{j+\frac{1}{2}}\frac{\bar{Q}^n_{j+1} - \bar{Q}^n_j}{\Delta x}\right) \tag{10}$$

where the quantity $\bar{h}^n_{j+1/2}$, $\bar{Q}^n_{j+1}\,\overset{*}{\square}u^n_j$ and will be discussed later below.

If we generalized the same momentum-conservative principle in two-layer system as in **[18]**, then **Equation (10)** can be generalized into the following approximation

$$(u_i\partial_x u_i)^n_{j+\frac{1}{2}} = \frac{1}{\bar{A}^n_{i,j+\frac{1}{2}}}\left(\frac{\bar{Q}^n_{i,j+1}\,\overset{*}{\square}u^n_{i,j+1} - \bar{Q}^n_{i,j}\,\overset{*}{\square}u^n_{i,j}}{\Delta x} - u^n_{i,j+\frac{1}{2}}\frac{\bar{Q}^n_{i,j+1} - \bar{Q}^n_{i,j}}{\Delta x}\right) \tag{11}$$

for $i = 1,2$.

Suppose we apply the same staggered arrangement as before, then we can approximate the unknown variables alternately on adjacent grid points. Thus, the fully discrete scheme for two-layer shallow flows as given below

$$\frac{A_{1,j}^{n+1} - A_{1,j}^{n}}{\Delta t} + \frac{Q_{1,j+1/2}^{n} - Q_{1,j-1/2}^{n}}{\Delta x} = 0 \tag{12}$$

$$\frac{u_{1,j+1/2}^{n+1} - u_{1,j+1/2}^{n}}{\Delta t} + (u\partial_x u)_{j+1/2}^{n} + \frac{1}{\sigma}\frac{\eta_{1,j+1}^{n+1} - \eta_{1,j}^{n+1}}{\Delta x} = 0 \tag{13}$$

$$\frac{A_{2,j}^{n+1} - A_{2,j}^{n}}{\Delta t} + \frac{Q_{2,j+1/2}^{n} - Q_{2,j-1/2}^{n}}{\Delta x} = 0 \tag{14}$$

$$\frac{u_{2,j+1/2}^{n+1} - u_{2,j+1/2}^{n}}{\Delta t} + (u\partial_x u)_{j+1/2}^{n} - \frac{h_{1,j+1}^{n+1} - h_{1,j}^{n+1}}{\Delta x} + \frac{1}{\sigma}\frac{\eta_{1,j+1}^{n+1} - \eta_{1,j}^{n+1}}{\Delta x} = 0 \tag{15}$$

where $\eta_{1,j} = h_{1,j} + h_{2,j} + d_j$. The later expression in **Equation (12)** - **Equation (15)** are obtained after using Euler Explicit w.r.t time derivative.

Furthermore, the upwind approximation for the fluxes $Q_{i,j+1/2}^{n}$ is given by the following

$$Q_{i,j+1/2}^{n} = {}^{*}h_{i,j+1/2}^{n}\, u_{i,j+1/2}^{n} \qquad {}^{*}Q_{i,j+1/2}^{n} = \begin{cases} Q_{i,j+1}^{n}, & u_{i,j+1/2}^{n} < 0 \\ Q_{i,j}^{n}, & u_{i,j+1/2}^{n} \geq 0 \end{cases}. \tag{16}$$

Whereas all other variables are calculated accordingly, as follows

$$\bar{A}_{i,j}^{n} = \frac{A_{i,j+1}^{n} + A_{i,j}^{n}}{2} \qquad \bar{Q}_{i,j}^{n} = \frac{Q_{i,j+1/2}^{n} + Q_{i,j-1/2}^{n}}{2} \tag{17}$$

$${}^{*}u_{i,j}^{n} = \begin{cases} u_{i,j-1/2}^{n}, & \bar{Q}_{i,j}^{n} \geq 0 \\ u_{i,j+1/2}^{n}, & \bar{Q}_{i,j}^{n} < 0 \end{cases}, \quad \text{for } i = 1,2. \tag{18}$$

The upwind approximation in **Equation (16)** is direct generalization of upwind for one layer.

When simulating the dam-break, dry area conditions are frequently occurred. To avoid the instability situation, we will use a basic wet-dry approach **[26]**, **[27]** in conjunction with a thin layer technique **[19]**. Thus, we resume here, the MCS scheme for the one-layer shallow flow is **Equation (7)** - **Equation (8)** whereas for the two-layer shallow flow is **Equation (12)** - **Equation (15)**

3. RESULT AND DISCUSSION

3.1 One Layer Shallow Flows

In this section we simulate a dam-break flow cases taken from **[22]**. A dam-break laboratory experiment is conducted in a rectangular horizontal channel, consist of a triangle obstruction as depicts in **Figure 2**. The channel dimensions are the following: 5.60 m long, 0.5 m wide, and 0.11 m high. The water barrier (gate) is situated 2.39 m upstream to produce a fluid reservoir, which is initially filled with water and has a height of $h_0 = 0.111\text{m}$. The triangle bottom obstruction with a height of 0.065 m, a length of 0.9 m, and bed slopes of 0.14 is placed 1.61m from the gate, forming a still water pool downstream of the channel. The downstream pool is 0.02m high at the right border is hard-wall. The simulations are conducted with; wet-dry threshold $= 0.0001$, thin film tolerance $= 0.0001$, spatial step $\Delta x = 0.025$, and CFL-like condition $= 0.1$. Initial condition for simulations is as follows: initial velocity $u(x,0) = 0$, initial flux $Q(x,0) = 0$.

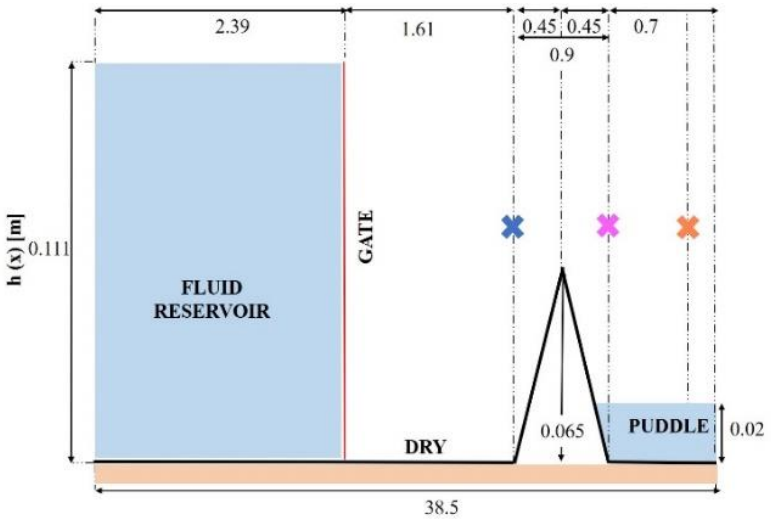

Figure 2. Dam-break experiment configurations across the triangle bottom obstacle. The top view of the channel, as well as the positions of the three gauges, are denoted by crosses: G1 (blue), G2 (magenta), and G3 (brown), which have been redrawn from [22].

The simulation results from our numerical approach (red) were shown alongside the experimental data (green) for the three-gauge sites plotted in **Figure 3** for Gauge 1-3 respectively. The experimental data can be found in **[22]**. The time series plot of water levels shows that the MCS scheme accurately predict the surface wave profile with RMSE $\leq 5\%$ and can anticipate the arrival of the shock fronts with sufficient accuracy, which is consistent with the experimental results in **[22]**. However, our model did not account for dispersive phenomena, considerable disparities were seen at Gauges 3, particularly in places where some hydraulic jump occurred. These disparities are also obtained in **[24]** which indicated that the model used was a hydrostatic without accommodating non-hydrostatic terms, thus inspiring us to recommend using the appropriate non-hydrostatic models as in our other published research on **[28]**.

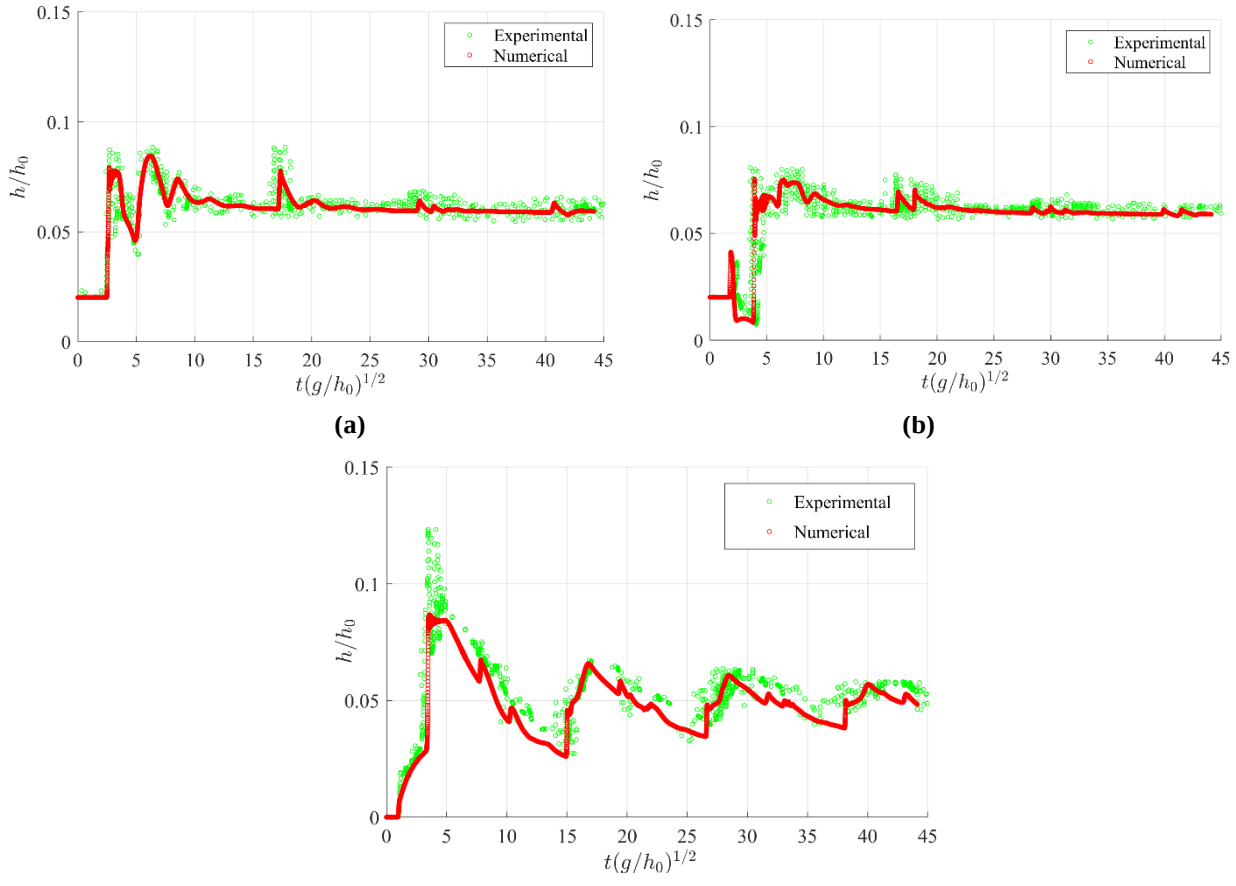

Figure 3. Time series plot of water levels, recorded at three gauges, data from experimental (green), numerical (red) for simulation with bottom triangular obstacles. (a) Gauge 1 G1, (b) Gauge 2 G2, and (c) Gauge 3 G3.

3.2 Two Layer Shallow Flows

In this section we simulate a steady sub-maximal exchange flow taken from [23]. Suppose we consider a rectangular channel with spatial domain $x \in [-3, 3]$. Here, the bottom topography is given by the following.

$$d(x) = \begin{cases} 0.5 - 0.125\left(\cos\frac{\pi x}{2} + 1\right)^2, & |x| \le 2 \\ 0.5, & \text{otherwise} \end{cases}, \tag{19}$$

Suppose the following parameters are used for computational simulation; ratio of the density $r = 0.9784$, the spatial and temporal step size of $\Delta x = 0.01$ and $\Delta t = 0.0005$, respectively. We consider the two-layer fluid system is initially steady-at rest with conditions; initial heights $h_1(x,0) = 1, h_2(x,0) = 0.5$, with zero velocities $u_1(x,0) = 0, u_2(x,0) = 0$. Further, we assume that the fluids in the upper and lower layers are moving in opposite directions or the flux ratio are $q_r = |Q_1/Q_2| = 1$. If we adopt the following boundary

$$\mathrm{h_1(-3,t)} = 0.2370,\ \mathrm{q_1(3,t)} = -0.1979\,,\mathrm{q_2(-3,t)} = 0.1979, \tag{20}$$

then, the initial two-layer system will undergo an adjustment process towards a steady state condition.

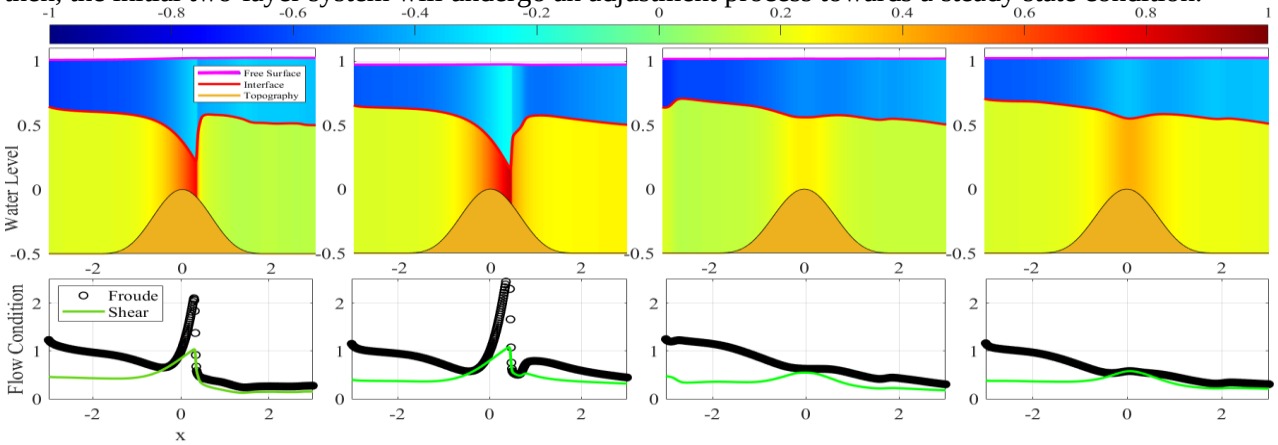

Figure 4. Sub-maximal exchange flow. From left to the right denoted water level evolution at subsequent time $t = 0.25, t = 0.75, t = 0.85, t = 1$. The flow condition plotted below are indicated composite Froude number (black circle) and shear (green line) along spatial domain x.

Under the influence of boundary conditions Equation (21), the interface is deformed and eventually develops into equilibrium, as depicted in Figure 4. As seen in Figure 4, the interface is higher than other areas on the left (upstream) side of the sill. The interface is distorted just above the sill and generates an upper convex shape due to the sill profile. In the downstream part, the interface gradually declines. Meanwhile the free surface is relatively flat during evolution. The horizontal velocity of the fluid in the two-layer system is depicted by the density color map. The blue color in the upper layer indicates that the fluid is flowing to the left (negative value on the color scale). Meanwhile, the yellow color at the bottom indicates that the fluids are going in another direction (to the right). In Figure 4 (below), the flow conditions are plotted. We observe the variation of the composite Froude number $G^2 \equiv F_1^2 + F_2^2 = \frac{u_1^2}{g'h_1} + \frac{u_2^2}{g'h_2}$ at subsequent times until a steady state is reached at $t = 1$ (see Figure 4). The Froude number is one just above the sill at $x = 0$ and on the far-left side at approximately $x \approx -2$. These two locations, where $G^2 \approx 1$, are referred to as control. During the evolution, the Froude number over the sill gradually changes, and the value $G^2 \approx 1$ is not maintained, indicating that control over the sill is lost. Additionally, the shear parameters $S = \frac{(u_1 - u_2)^2}{g'(h_1 + h_2)}$ of the flow conditions are less than 1 on both the right and left sides of the sill. Further, the flux at steady condition $|\mathrm{q_{1s}}| = \mathrm{q_{2s}} = 0.1979$ which is less than threshold value of maximal exchange fluxes $q = 0.2081$, see [23] for detailed description. This circumstance suggests that a steady state in the form of an sub-maximal exchange flow without sill control has been achieved, see [23]. Furthermore, the free surface remains flat at a constant height equal to one.

4. CONCLUSIONS

We have successfully re-examined and implemented the MCS scheme as a computational model to solve various cases involving one and two-layer shallow flows. The study emphasizes the robustness of their computational technique in handling complex flow scenarios, demonstrating its ability to effectively replicate the generation and propagation of free surface waves due to the dam-break in one layer and sub-maximal behavior in a two-layer fluid system. The capability of our scheme is validated by conducting numerous numerical simulations, examining various scenarios involving one-dimensional dam-break through triangular obstacles in open channels and steady sub-maximal exchange. The simulation results show good agreement with the experimental data and the theoretical aspect as in the literature. This satisfying assessment indicates that our proposed numerical model is not only powerful but also efficient, meaning it provides accurate results without unnecessary computational overhead. This alignment between simulated and experimental or theoretical aspects underscores the accuracy and reliability of our scheme. Furthermore, the MCS scheme is suitable for practical needs involving various flow situations both one- and two-layer cases.

ACKNOWLEDGMENT

Financial funding of this research was supported by DIPA PNBP Universitas Udayana TA- 2023 No. : B/1.612/UN14.4.A/PT.01.03/2023

REFERENCES

[1] D. Bourgault, P. S. Galbraith, and C. Chavanne, “Generation of internal solitary waves by frontally forced intrusions in geophysical flows,” *Nat. Commun.*, vol. 7, 2016, doi: 10.1038/ncomms13606.
[2] M. J. Castro, J. A. García-Rodríguez, J. M. González-Vida, J. Marías, C. Parés, and M. E. Vázquez-Cendón, “Numerical simulation of two-layer shallow water flows through channels with irregular geometry,” *J. Comput. Phys.*, vol. 195, no. 1, pp. 202–235, 2004, doi: 10.1016/j.jcp.2003.08.035.
[3] M. J. Castro, J. A. García-Rodríguez, J. M. González-Vida, J. Macías, and C. Parés, “Improved FVM for two-layer shallow-water models: Application to the Strait of Gibraltar,” *Adv. Eng. Softw.*, vol. 38, no. 6, pp. 386–398, 2007, doi: 10.1016/j.advengsoft.2006.09.012.
[4] S. R. Pudjaprasetya, V. M. Risriani, and Iryanto, “Numerical simulation of propagation and run-up of long waves in U-shaped bays,” *Fluids*, vol. 6, no. 4, pp. 1–13, 2021, doi: 10.3390/fluids6040146.
[5] K. R. Helfrich, “Time Dependent Two-Layer Hydraulic Exchange Flows,” *J. Phys. Oceanogr.*, vol. 25, no. 3, pp. 359–372, 1995, doi: 10.1175/1520-0485(1995)025<0359:TDTLHE>2.0.CO;2.
[6] P. Brandt, W. Alpers, and J. O. Backhaus, “Study of the generation and propagation of internal waves in the Strait of Gibraltar using a numerical model and synthetic aperture radar images of the European ERS 1 satellite,” *J. Geophys. Res. C Oceans*, vol. 101, no. C6, pp. 14237–14252, 1996, doi: 10.1029/96JC00540.
[7] P. Brandt, A. Rubino, W. Alpers, and J. O. Backhaus, “Internal waves in the Strait of Messina studied by a numerical model and synthetic aperture radar images from the ERS 1/2 satellites,” *J. Phys. Oceanogr.*, vol. 27, no. 5, pp. 648–663, 1997, doi: Numerical study of cascading dam-break characteristics using SWEs.
[8] S. Dai, Y. He, J. Yang, Y. Ma, S. Jin, and C. Liang, “Numerical study of cascading dam-break characteristics using SWEs and RANS,” *Water Supply*, vol. 20, no. 1, pp. 348–360, Feb. 2020, doi: 10.2166/ws.2019.168.
[9] Y. Zhang and P. Lin, “An improved SWE model for simulation of dam-break flows,” *Proc. Inst. Civ. Eng. Water Manag.*, vol. 169, no. 6, pp. 260–274, 2016, doi: Dam-break flows during initial stage using SWE and RANS approaches.
[10] H. Ozmen-Cagatay and S. Kocaman, “Dam-break flows during initial stage using SWE and RANS approaches,” *J. Hydraul. Res.*, vol. 48, no. 5, pp. 603–611, Oct. 2010, doi: 10.1080/00221686.2010.507342.
[11] P. V. Swastika, M. Fakhruddin, S. Al Hazmy, S. Fatimah, and A. De Souza, “A novel technique for implementing the finite element method in a shallow water equation,” *MethodsX*, vol. 11, p. 102425, Dec. 2023, doi: 10.1016/j.mex.2023.102425.
[12] R. Iacono, “Analytic solutions to the shallow water equations,” *Phys. Rev. E*, vol. 72, no. 1, p. 017302, Jul. 2005, doi: 10.1103/PhysRevE.72.017302.
[13] M. J. Castro *et al.*, “The numerical treatment of wet/dry fronts in shallow flows: Application to one-layer and two-layer systems,” *Math. Comput. Model.*, vol. 42, no. 3–4, pp. 419–439, 2005, doi: 10.1016/j.mcm.2004.01.016.
[14] B. Arry Sanjoyo, M. Hariadi, and M. H. Purnomo, “Stable Algorithm Based On Lax-Friedrichs Scheme for Visual Simulation of Shallow Water,” *Emit. Int. J. Eng. Technol.*, vol. 8, no. 1, pp. 19–34, Jun. 2020, doi: 10.24003/emitter.v8i1.479.
[15] A. Arakawa, “Computational Design for Long-Term Numerical Integration of the Equations of Fluid Motion: Two-Dimensional Incompressible Flow. Part I,” *Journal of Computational Physics*, vol. 1, no. 1, pp. 119–143, 1997.
[16] G. S. Stelling and S. P. A. Duinmeijer, “A staggered conservative scheme for every Froude number in rapidly varied shallow water flows,” *Int. J. Numer. Methods Fluids*, vol. 43, no. 12, pp. 1329–1354, 2003, doi: 10.1002/fld.537.
[17] P. V. Swastika, S. R. Pudjaprasetya, L. H. Wiryanto, and R. N. Hadiarti, “A momentum-conserving scheme for flow simulation in 1D channel with obstacle and contraction,” *Fluids*, vol. 6, no. 1, p. 26, 2021, doi: 10.3390/fluids6010026.

[18] P. V. Swastika and S. R. Pudjaprasetya, "The Momentum Conserving Scheme for Two-Layer Shallow Flows," *Fluids*, vol. 6, p. 346, 2021, doi: 10.3390/fluids6100346.
[19] N. Erwina, D. Adytia, S. R. Pudjaprasetya, and T. Nuryaman, "Staggered Conservative Scheme for 2-Dimensional Shallow Water Flows," *Fluids*, vol. 5, no. 3, pp. 1–18, 2020, doi: 10.3390/fluids5030149.
[20] S. R. Pudjaprasetya and R. Sulvianuri, "The momentum conservative scheme for simulating nonlinear wave evolution and run-up in U-shaped bays," *Jpn. J. Ind. Appl. Math.*, vol. 40, no. 1, pp. 737–754, Jan. 2023, doi: 10.1007/s13160-022-00549-4.
[21] P. V. Swastika, S. R. Pudjaprasetya, and N. Subasita, "Numerical simulation of two-layer shallow water flows; Exchange Flow in Lombok Strait," *East Asian J. Appl. Math.*, vol. Accepted and to be appear 2025 (in Private Communication).
[22] S. Soares-Frazão, "Experiments of dam-break wave over a triangular bottom sill," *J. Hydraul. Res.*, vol. 45, no. sup1, pp. 19–26, Dec. 2007, doi: 10.1080/00221686.2007.9521829.
[23] D. M. Farmer and L. Armi, "Maximal two-layer exchange over a sill and through the combination of a sill and contraction with barotropic flow," *J. Fluid Mech.*, vol. 164, no. 10, pp. 53–76, 1986, doi: 10.1017/S002211208600246X.
[24] I. Magdalena, A. A. A. Hariz, M. Farid, and M. S. B. Kusuma, "Numerical studies using staggered finite volume for dam break flow with an obstacle through different geometries," *Results Appl. Math.*, vol. 12, p. 100193, 2021, doi: 10.1016/j.rinam.2021.100193.
[25] S. R. Pudjaprasetya and I. Magdalena, "Momentum conservative schemes for shallow water flows," *East Asian J. Appl. Math.*, vol. 4, no. 2, pp. 152–165, 2014, doi: 10.4208/eajam.290913.170314a.
[26] G. S. Stelling, A. K. Wiersma, and J. B. T. M. Willemse, "Practical Aspects of Accurate Tidal Computations," *J. Hydraul. Eng.*, vol. 112, no. 9, pp. 802–816, 1986, doi: 10.1061/(asce)0733-9429(1986)112:9(802).
[27] A. Balzano, "Evaluation of methods for numerical simulation of wetting and drying in shallow water flow models," *Coast. Eng.*, vol. 34, no. 1–2, pp. 83–107, 1998, doi: 10.1016/S0378-3839(98)00015-5.
[28] K. Dharmawan, P. V. Swastika, G. K. Gandhiadi, and S. R. Pudjaprasetya, "A Non-hydrostatic Model for Simulating Dam-Break Flow Through Various Obstacles," *MENDEL*, vol. 30, no. 1, pp. 33–42, Jun. 2024, doi: 10.13164/mendel.2024.1.033.